Effect of the irradiation dose on the luminescence emission of a Mg–rich phyllosilicate

Article *in* Journal of Radioanalytical and Nuclear Chemistry · June 2015

DOI: 10.1007/s10967-015-4229-8

4 authors, including:

V. Correcher
Centro Investigaciones Energéticas, Medioa…
165 PUBLICATIONS **1,306** CITATIONS
SEE PROFILE

Yamilet Lazcano
Universidad Autónoma de Nayarit
31 PUBLICATIONS **203** CITATIONS
SEE PROFILE

Javier Garcia-Guinea
The National Museum of Natural Sciences
337 PUBLICATIONS **1,964** CITATIONS
SEE PROFILE

J Radioanal Nucl Chem (2016) 307:1287–1293
DOI 10.1007/s10967-015-4229-8

Effect of the irradiation dose on the luminescence emission of a Mg-rich phyllosilicate

V. Correcher[1] · Y. Rodriguez-Lazcano[1] · R. Gomesdarocha[1] · J. Garcia-Guinea[2]

Received: 23 March 2015 / Published online: 20 June 2015

Abstract This paper reports on the thermoluminescence and cathodoluminescence behaviour of a well-characterized sepiolite ($Si_{12}Mg_8O_{30}(OH)_4(OH_2)_4{\cdot}8H_2O$). Both natural and induced thermoluminescence curves display a complex emission suggesting a continuum in the trap distribution involving multiorder kinetics. UV–IR cathodoluminescence spectral emission shows five wavebands at 330, 400 and 440 (associated with structural defects, $[AlO_4]$ or non-bridging oxygen hole centers) and 520 and 770 nm (linked to point defects). This daily-use material, that is of interest since could be employed for personal dosimetry in the case of radiation accident or radiological terrorism where conventional monitoring has not been established, were never investigated before.

Keywords Sepiolite · Thermoluminescence · Cathodoluminescence · Accidental dosimetry

Introduction

Sepiolite ($Si_{12}Mg_8O_{30}(OH)_4(OH_2)_4{\cdot}8H_2O$) is a complex hydrated magnesium silicate clay mineral that can absorb its own weight of water and other liquids [1]. Due to this property and because is a non-flammable material, sepiolite is used for a wide variety of industrial applications such as (i) rheological additives for aqueous or organic systems, (ii) carriers for chemicals, (iii) moisture control or (iv) many different household uses (for moisture control, containment of accidental liquid spillages, use in ashtrays to avoid smoke smell, control of liquid leakages and odours in dustbins and cat litters to absorb pet urine and has a dehydrating effect on solid dregs which reduces bad odours and inhibits bacteria proliferation) [2, 3]. It is precisely for this last application, which makes this ubiquitous material of interest for dosimetric purposes in case of radiation accident or radiological terrorism where conventional monitoring has not been established. Similar to other phyllosilicates (lepidolite [4] or kaolinite [5, 6]), sepiolite could exhibit useful luminescence-dosimetric properties, although this property has been scarcely studied. Only Bulur [7] performed a preliminary study considering the optically stimulated luminescence emission of a Turkish sepiolite. However, to the best of our knowledge, the cathodo- (CL) and thermoluminescence (TL) characterization of this material were never investigated up to now. TL is based on the emission of light from a solid sample (insulator or semiconductor) when the sample is heated after being irradiated by X-rays, gamma rays, beam of electrons, cosmic rays, etc. The ionizing radiation absorbed by the material at room temperature (RT) induces free electrons that become trapped in the lattice defects of the material (point defects, vacancies, Schottky defects, Frenkel defects, dislocations, planar defects, etc.) It is accepted that in this process such electrons will be trapped for long periods of time while the material is stored at RT. When the temperature is increased, the electrons can release from the traps and in a recombination process they reach more stable energies with emission of photons and the TL signal is recorded as a function of temperature or wavelength. The luminescent intensity and the shape of this glow curve are functions of the radiation absorbed dose and heating rate [8]. CL is a process whereby light is created from an

✉ V. Correcher
v.correcher@ciemat.es

[1] CIEMAT, Av. Complutense 22, 28040 Madrid, Spain

[2] CSIC. Museo Nacional Ciencias Naturales, José Gutiérrez Abascal 2, 28006 Madrid, Spain

energetic electron beam and supplies data about transient defects after irradiation on the surface of the lattice. Therefore, CL is used in the identification of the migration and diffusion of some luminescent centres from the emission bands [9]. Both TL and CL provides information about the trapped charge recombination sites related to metastable defects inside the lattice depending on whether the detrapping process is due to heat or electron exposure, respectively. All factors involved in the luminescence phenomena (i.e. lifetime, efficiency, emission spectra, etc.) depend directly on the crystalline phase, which is mainly influenced by pressure and temperature. Thus, small variations in the lattice structure due to the presence of inclusions, impurities, substituted ions or surface defects in ppm concentrations show changes in the intensity and wavelength position the emission spectra [10]. Supergenic sepiolite is found as a secondary mineral associated with serpentine and sedimentary sepiolite and appears linked to opal and palygorskite, e.g., in the Tagus river basin in which we collected samples (Batallones hill, Madrid). The sepiolite structure is formed by (i) tetrahedral silicon sheets, with an apical oxygen inverted, bound to octahedral magnesium sheets (typical T-O-T structure of phyllosilicates) [11, 12], (ii) tunnels in the inner of the particle and (iii) channels (open tunnels in the external surface) [13, 14]. This clay can be formed by hydrothermal processes or by sedimentation [15], although the most accepted mechanism for its formation is by the direct precipitation from solutions containing silica and magnesium [16]. Considering the complex process of formation of this clay, one can easily guess the structure of sepiolite containing intrinsic (i.e., lattice defects), extrinsic (i.e., impurities) as well as structural defects in the lattice that are responsible of the luminescence emission. This paper is basically focused on the study of the luminescence (CL and TL) characterization of a sepiolite (analyzed by environmental scanning electron microscope (ESEM), X-ray fluorescence (XRF) and X-ray diffraction (XRD) techniques) collected from the Batallones (Madrid, Spain).

Experimental

The sepiolite collected from the Batallones, was examined on an ESEM microscope, of FEI Company, settled in the Spanish National Museum of Natural Sciences (MNCN). It is a low-vacuum ESEM with a large sample chamber wide enough to hold large samples without the sputtered covering onto sample. The chemical composition was determined by XRF using a PHILIPS PW-1404 spectrometer with a Sc-Mo tube, Ge, LIF220, LIF200, PE and TLAP analyzer crystals and Super-Q manager from Panalytical-Spain as analytical software. For the XRF measurements, sepiolite pellets of 8 g of milled sample with 0.1 g of elbacite were pressed under 20 TM and dried at 40 °C in a climatic chamber. The bulk chemical analysis of the sample is: SiO_2 62.11 %, Al_2O_3 0.65 %, Fe_2O_3 (total) 0.26 %, MnO 0.02 %, MgO 25.41 %, CaO 0.12 %, K_2O 0.11 %, TiO_2 0.06 %, P_2O_5 0.01 %, Loss on ignition 11.25 %. Powdered sample of sepiolite was sent to Acme Analytical Labs in Vancouver (Canada) for a multi-element ICP-MS package (Acme method VAN4A4B 32) for whole analysis trace elements with previous preparation R200-250 29 which implies crush split and pulverize 250 g sample up to 200 meshes. The content of impurities (in ppm) is: Zr 24, Rb 9, Sr 4, Ni 2, Co 6, Ba 63, V 47, Nb 4, Cs 34, U 12, Tl <0.1. The XRD analyses were performed using XPOWDER software which also allows a full duplex control of the Philips PW-1710 = 00 diffractometer (Kent, United Kingdom) using the CuK_α radiation with a Ni filter and a setting of 40 kV and 40 mA. The CL spectra were measured using a Gatan MonoCL3 detector with a PA-3 photomultiplier tube attached to the ESEM model XLS30. The detector covers a spectral range of 250–1000 nm being most sensitive in the blue parts of the spectrum. The samples were placed on polished slabs, at low-vacuum mode without coating to keep open way out to the CL emission. The emission of the samples was collected and amplified using a retractable parabolic diamond mirror and a photomultiplier tube. The distance between the sample and the bottom of the CL mirror assembly was 15 mm. The excitation for CL measurements was provided at 25 kV electron beam.

The stability of TL signal has been studied for natural non-irradiated samples (NTL) using a preheat technique that consists of linear heating of the samples up to a temperature T_{stop} followed by quick cooling to RT and final readout (up to 500 °C) to record the whole remaining TL glow curve [8], where thermal preheating varies from 250 to 360 °C. The TL measurements were performed using an automated Risø TL reader model TL DA-12 provided with an EMI 9635 QA photomultiplier [17]. The emission was observed through a blue filter (a FIB002 of the Melles-Griot Company) where the wavelength is peaked at 320–480 nm; FWHM is 80(16) nm and peak transmittance (minimum) is 60 %. The TL reader is also provided with a $^{90}Sr/^{90}Y$ source with a dose rate of 0.012 Gy s^{-1} calibrated against a ^{137}Cs photon source in a secondary standard laboratory [18]. The sample was carefully powdered with an agate pestle and mortar to avoid triboluminescence [19]. All the TL measurements were performed using a linear heating rate of 5 °C s^{-1} from RT up to the corresponding temperature in a N_2 atmosphere. Aliquots of 5.0(1) mg of the sample were used for TL measurements.

Results and discussion

ESEM and XRD characterization

Unlike other claystone materials, i.e. layered phyllosilicates, sepiolite appears as porous needle-like spheres with channels cavities displaying fiber morphology (Fig. 1). The structure is mainly formed by tetrahedral and octahedral sheets giving rise to zeolitic channels (containing zeolitic water) and open channels. Both the structural tunnels and channels run parallel to the fiber inducing a high surface area and porosity that are responsible for its big absorption capacity for liquids [20].

As observed in Fig. 1, this sample exhibits straight and rigid fibers in spheres, slightly curly intermediate fibers oriented in all directions, with lengths between 1 and 10 μm; it is in good agreement with the previous study performed by Garcia-Romero and Suarez [14]. This complex structure can be easily modified by the effect of the thermal treatments where a heating from RT to 500 °C induces changes in the lattice that can be associated with the loss of (i) hygroscopic zeolitic water molecules (designated as H_2O) and (ii) coordinated or crystallographically bound water molecules [designated as $(OH_2)_4$]. The variation in the lattice of preheated sepiolite at 300, 400 and 500 °C has been studied by means of XRD technique (Fig. 2).

As is observed, all the peaks are fairly well-correlated with the studies previously reported for this material [21]. The main reflection peak in non-preheated sepiolite appears at $2\theta = 7.2°$ that corresponds to the (110) plane. The intensity of this peak of sepiolite crystal is twice as high as other crystal planes, indicating that crystallization degree of sepiolite crystal planes (110) is significantly higher than that of other crystal planes, which becomes the foundation of sepiolite mineral crystal as appreciated in the 25 °C X-ray pattern. Variances in the peak position as well as in its width and relative intensity have been found in different samples linked to its compositions and structural properties [11, 13]. Increasing the heating temperature modifies the XRD pattern up to 500 °C; i.e., some peaks change the relative intensity as is shown in Fig. 2. However, the most drastic variation is observed circa 400 °C where the maximum peaked at 7.2° disappears mainly due to the formation of the anhydrous sepiolite; the progressive loss of zeolitic water releases spaces in the channels giving rise to a reduction in the unit-cell volume [11, 22]. Thermal treatment at 500 °C produces the complete dehydration of both, the hygroscopic zeolitic H_2O and the coordinated OH_2. According to Miura et al., [23] long-term thermal treatments changed the composition, morphology, crystal structure, and surface area of the sepiolite. The morphological changes were possibly related to the modifications in the sepiolite crystal structure and/or formation of Mg-rich compounds in this phyllosilicate after the leaching of the Si^{4+} ions, as well as the aforementioned dehydration process. Such effect has been previously described by thermal gravimetric analysis (TGA) by Tuler et al., [21] who demonstrate how temperatures below 300 °C give rise to the loss of zeolitic and adsorbed water molecules while samples heated in the range of 300–600 °C induce the loss of the coordinated water.

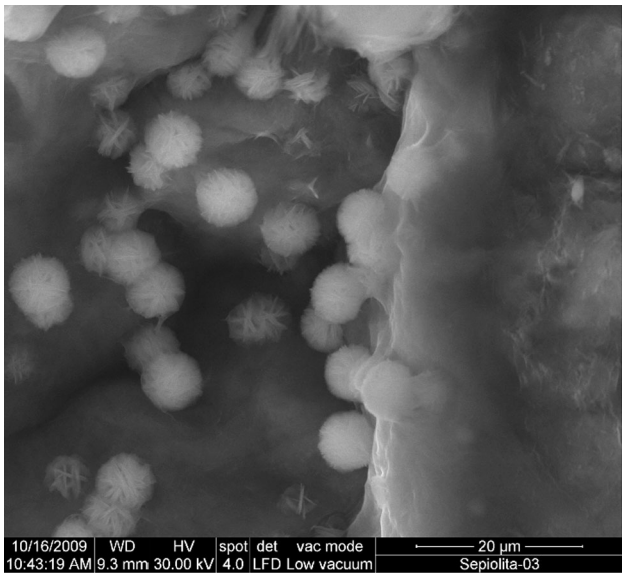

Fig. 1 Environmental scanning electron microscope (ESEM) image of straight and rigid fibers in spheres of sepiolite with lengths between 1 and 10 μm sample

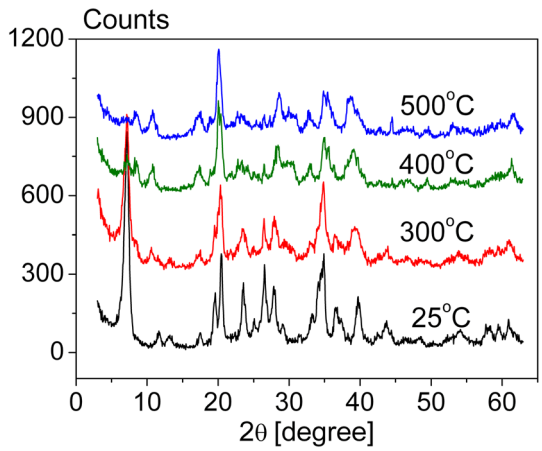

Fig. 2 X-ray profiles of sepiolite from room temperature (25 °C) to 500 °C showing the removal of the 7.2° (2θ) peak and changes in the position, width and relative intensity of the peak due to the formation of the anhydrous sepiolite

Cathodo- and UV-blue thermoluminescence behaviour

CL spectral emission of the sepiolite, in the UV–IR region (from 200 to 1000 nm), displays three narrow maxima

peaked at 330, 400, 440 and two wider peaks at 520 and 770 nm (Fig. 3).

According to Correcher et al., [24] low-energy emissions should be more associated with point defects and low wavebands to structural or intrinsic defects in the lattice. In this sense, the 330 nm emission peak, that is very common in the luminescence spectra of silicates, can be linked to the lattice stress in their 3D framework silicon–oxygen structure [25]. These Si–O strained structures could include some non-bridging oxygen centers (NBOC) or silicon vacancy-hole centers and Si–O bonding defects. Therefore, we can speculate that sepiolite, as many other types of clays, includes such centers which seems to be responsible for this common 330 nm CL emission [26]. Many Si–O bonds undergo an additional stress due to different processes, namely dehydration or dehydroxylation or both processes, involving losses of H_2O, with hydrogen atoms bonded to the lattice, or breaking of hydroxyl groups, also bonded to the silicate framework. The emission at 400 nm, as suggested by Itoh and coworkers [27], can be attributed to $[AlO_4]^-$ centers through electron–hole mechanisms. The exposure to the electron beam induces the ionization of the oxygen atoms closed to the aluminum giving rise to electron–hole pairs. It should generate $[AlO_4/h^+]$ centers in which alkali atoms (M^+) diffuse from the lattice away. The alkali should join to an electron to become neutral in the crystal network. These $[AlO_4/h^+]$ centers combined with electrons are the origin of the $[AlO_4]°$ centers. At the same time, these centers can be associated with M^+ or electron–holes producing $[AlO_4/M^+]$ and $[AlO_4/h^+]$ centers, respectively. The production–annihilation of luminescent $[AlO_4]°$ centers could be analyzed in terms of ionic self-diffusion. In this case, the electron beam radiation should increase the ionicity of the Si–O bonds modifying the ground state where each Si atom has four valence electrons and each O atom six valence electrons, implying that O states would exceed in number Si states by 3:1 considering

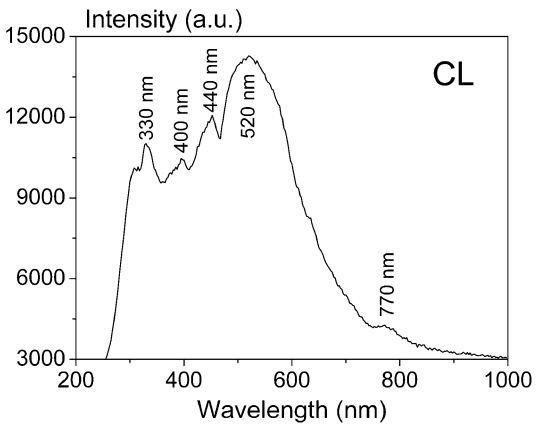

Fig. 3 UV–IR CL spectral emission of the sepiolite

atoms widely separated. The resulting centers $[AlO_4/M^+]$, $[AlO_4/h^+]$ and $[AlO_4]°$ are formed during self-diffusion processes through the bulk and interfaces due to changes in the temperature of the lattice [28]. XRF analysis shows the presence of a content of 0.65 % of Al in the studied sample that seems to be enough to produce such UV-blue emission. The waveband at 440 nm can be associated with radiation-induced defects, i.e. O^- color centers [29] in agreement with EPR (electron paramagnetic resonance) spectroscopy results [30]. The band emission in the range 400–500 nm can be associated with (i) the effect of the irradiation that induces the formation of –O–O– type defects or O_2^- intrinsic defects [9] and (ii) radiative recombination of self-trapped excitons (STE) due to the radiolysis of oxygen bonds; the gain in energy is due to the interaction between an electron in the conduction band and a hole in the valence band along the lattice. The interaction of free excitons with phonons gives rise to its localization in the lattice (so-called self-trapping) inducing this blue emission [9, 31, 32].

The green emission appearing at 520 nm can be attributed to the presence of Mn^{2+} (0.02 % estimated by XRF) substitutions in Mg^{2+} sites in the sepiolite lattice [31, 32] that seems to be characteristic of a d^5 electronic configuration [33]. However, taking into account the broad shape of this green band could mask additional spectra of accessorial uranyl groups (12 ppm of U^{4+}) that substitutes to Si^{4+} [34] and/or other cations, e.g., thallium (<0.1 ppm), with maxima peaks in the 520 nm spectral surroundings [35]. The red band at 770 nm, is produced when the irradiation from the electron beam (in this case) reduces some Fe^{3+} to Fe^{2+} impurities [36]. Iron atoms (0.26 % in the sample) can be substituted at Si (tetrahedrally coordinated) sites in the silicate lattice, acting as recombination sites for holes or electrons, depending on the valence. Such electron beam on the sample could induce a charge transfer between O^{2-} and Fe^{3+} [37]. The probable reaction can be described in two steps namely, (i) a reduction process where electrons are trapped by the ferric ions, creating hole centres and (ii) holes are trapped at hole centres by an oxidation process of ferrous ion (Fe^{2+}). There is an intermediate step where the excited energy state of the Fe^{3+} is created that is followed by a relaxation to the ground state producing the emission of a photon in the red region of the spectrum due to a $^4T_1(G) \rightarrow {}^6A_1(S)$ transition [38].

Figure 4a shows changes in the UV-blue TL glow curves of non-irradiated samples after different thermal pretreatments in a range from 250 to 360 °C. The origin of the natural TL (NTL) glow curve, which consists of an intense broad peak centred at 320 °C, is related to traps that are not easily bleached by optical processes. This emission is moving continuously towards higher temperatures when preheating treatment (T_{stop}) ranges from 250 °C in steps of

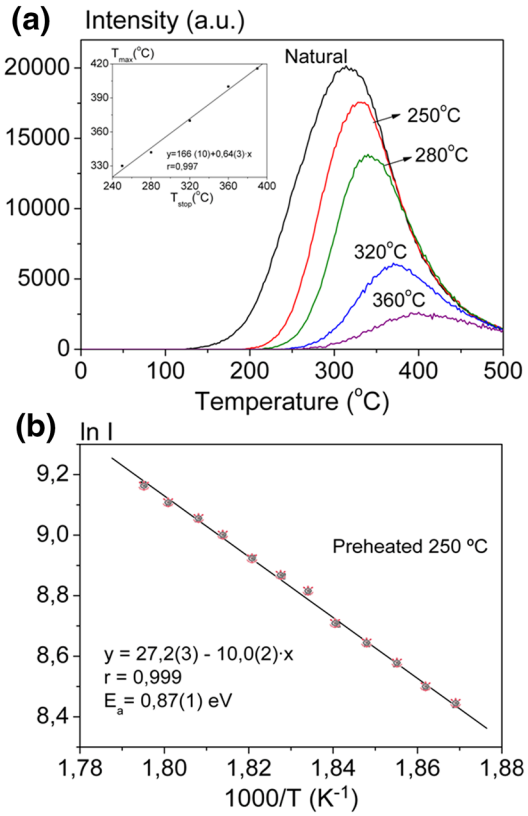

Fig. 4 **a** TL glow curves of non-irradiated sepiolite samples after different preheating in a range 250–360 °C. The *inset* shows the shift of the maximum TL temperature (T_{max}) versus the preheating temperature (T_{stop}) along with the linear fitting. **b** Arrhenius plot of the low-T side of the 230 °C preheated TL curve of sepiolite where the $E_a = 0.87(1)$ eV

30–40 °C; the intensity of the maxima decreases similarly to the peak area. The inset corresponds to the shift of the maximum TL temperature (T_{max}) against the preheating temperature (T_{stop}). As is appreciated, the mathematical fitting indicates a lineal evolution that is linked to a group of components, where the fitting regression coefficient (r) is 0.997. This behaviour should correspond to a continuous trap distribution also observed in other different natural materials previously studied in our laboratory (phyllosilicates –lepidolite- [4], K-rich aluminosilicate, leucite [31, 32]) and polymineral materials (meteorites [39]).

This assumption is supported since NTL glow emission display curves with a trap structure that cannot be explained employing the commonly accepted model based on the discrete trap distribution. It was not possible to determine some physical parameters such as trap-energies or pre-exponential factors after being analysed in terms of both first (corresponding to the cases where the intensity of the TL is proportional to the concentration of thermally released charges) and second order kinetics equations (where the thermally released charges are retrapped at least once before the recombination process). The best fitting parameters obtained, based on the value of the factor of merit, were unsatisfactory. Therefore, due to this complexity of the TL glow curves one could assume a structure of a continuous trap distribution involving multiorder kinetics. Consequently, the typical shift of the maximum peak towards higher temperatures is observed just with a change in the shape and intensity of the TL distribution depending on the thermal pre-treatment employed. Such behavior could be linked to consecutive breaking and linking of bonds of Al–O, Fe–O, Mg–O including dehydroxylation, dehydration (of both zeolitic and coordinated water molecules) and redox reactions in sepiolite.

Table 1 shows the activation energy (E_a) calculated for natural sepiolite preheated at different temperatures (T_{stop}) in the range 250–360 °C by means of the initial rise (IR). This method is based on the hypothesis that occupancies of the relevant states remain almost constant for the lowest temperature side of the TL peak and, consequently, this side of the peak will follow an exponential dependence regardless of the kinetic order and the applicability of the quasi-equilibrium approximation $I_{TL} \propto \exp(-E_a/kT)$, where I_{TL} is the TL intensity, k is the Boltzmann's constant and T is the temperature. Therefore, in the Arrhenius plot ($\ln I_{TL}$ vs $1/T$), the E_a can be obtained from the slope (angular coefficient) $-E_a/k$, irrespectively of any other kinetic parameter [40–42]. Figure 4b displays the Arrhenius plot of the low-T side of the NTL UV-blue emission of the 250 °C preheated sample with the experimental data marked on the fitting line where the E_a is 0.87(1) eV and the estimated value of correlation coefficient (r) is 0.999, indicating a good fitting.

The dose dependence of the TL emission from this material was also investigated in the range of 1–8 Gy (Fig. 5). Irradiated sepiolite aliquots exhibits a TL sensitivity similar to other phyllosilicates studied in our lab under the same conditions (kaolinite [6] or lepidolite [4], although quite less intensity luminescence signal respect to

Table 1 Calculation of the activation energy (E_a) values by initial rise (IR) method resulting of the analysis of natural TL glow curve of sepiolite by means of the T_{stop} method

T_{stop} (°C)	Range (°C)	a	b	Ea (eV)	r
0	202–230	25.1 (2)	8.2 (1)	0.70 (1)	0.999
250	262–284	27.2 (3)	10.0 (2)	0.87 (1)	0.999
280	260–284	34.3 (5)	14.4 (3)	1.24 (2)	0.998
320	280–308	32 (1)	14.5 (6)	1.25 (5)	0.990
360	264–340	30 (1)	14.4 (7)	1.24 (6)	0.962

a is a coefficient of the equation, b corresponds to the slope (angular coefficient) and r is the correlation coefficient from the fitting of an equation of the sort $y = a + bx$

The number into parentheses corresponds to the uncertainties associated with the measurements

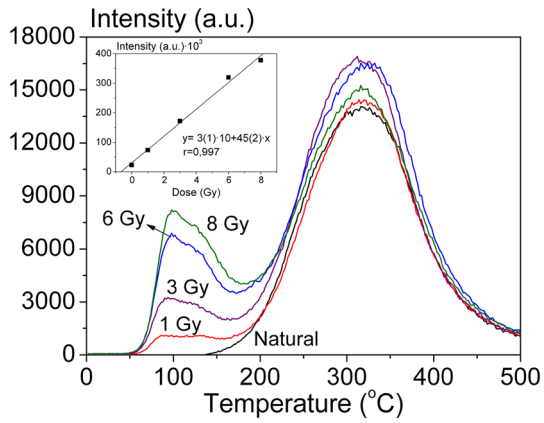

Fig. 5 Dose dependence in a range of 1–8 Gy of the TL glow curve. The inset shows the good linearity ($r = 0.997$) of the TL glow emission with the dose between 50 and 170 °C

other silicates (microcline [43] or albite [44]). Induced TL glow curve displays (i) a higher temperature broad maximum peaked at 320 °C that is hardly affected by the irradiation and (ii) a lower temperature group of components in the range of 50–170 °C, with a very complex structure, that is directly related to the radiation effect. The inset of Fig. 5 depicts the evolution of the whole area of the induced TL 100 °C peak in the above-mentioned range in which the dose shows a good linearity ($r = 0.997$) fitted to an equation of the sort $y = y_0 + bx$, where y corresponds to the intensity of the TL signal, x is the given dose and y_0 is a coefficient of the equation. In the studied range of dose, usually employed in the fields of retrospective dosimetry and dating, no saturation has been detected for any group of components up to 200 °C. It means that the number of the trapped charges is low and the number of recombination centres high, then the luminescence is proportional to the number of the charges being de-trapped. On the other hand, the blue emission from 200 °C onwards displays saturation behaviour because the concentration of the recombination centres is low, and the interaction between the relative proportion of trapped charges, recombination centres and the rate of charge de-trapping give rise to a complex competition. Despite radiation may induce displacement of lattice ions or to produce electron defects involving changes in the valence state of impurities atoms and consequently changes in the spectral composition. No modifications could be appreciated in the blue TL curves when increasing the dose.

Conclusions

Sepiolite, collected from Batallones Hill (Madrid, Spain), shows straight and rigid fibres modelling spheres with lengths from 1 up to 10 μm, losses both zeolitic and coordinated or crystallographically bound water molecules with thermal treatments up to 500 °C. The CL emission spectrum shows five maxima centered at 330, 400, 440 (associated with structural defects, i.e. non-bridging oxygen hole centers or [AlO_4] centers) and 520 and 770 nm (related, respectively, with the presence of point defects associates with Mn^{2+} and Fe^{3+} 0.02 and 0.26 % respectively). The extensive green CL band can be hiding extra spectra of accessorial uranyl groups and/or other cations, e.g., thallium, with maxima peaks sited near such 520 nm spectral position. Thermal treatments performed on the sample induce consecutive breaking and linking of bonds of Al-O, Fe–O including dehydroxylation, dehydration (of both zeolitic and coordinated water molecules) and redox reactions that have been detected by means of (i) XRD (with the disappearance of the maximum peaked at 7.2°) and (ii) TL. The tests of thermal stability at different temperatures performed on the main group of components peaked at 320 °C (corresponding to the UV-blue natural TL emission) confirm a continuous trap distribution. It could be appreciated how the application of the T_{stop} method (with thermal pretreatments in the range of 250–360 °C) gives rise to a progressive shift of the position of the maximum, as well as the decrease of the peak area. This behaviour can be associated with a successive emptying of the traps and could be linked to the aforementioned chemical and structural processes. The estimation of the activation energy (E_a), by means of the IR method, displays a gradual increase in value from 0.70 to 1.25 eV, that confirm the previous hypothesis about the trap distribution. The dose dependence of the 400 nm TL intensity of sepiolite shows an excellent linearity in the range of 1–8 Gy. These preliminary results on the luminescence properties of sepiolite, allow us to think on the potential use of this material, for instance, in the field of retrospective dosimetry; nevertheless further works are necessary to confirm such assertion.

Acknowledgments This work was partially supported by the CNPQ, program *Ciências sem Fronteiras* (238437/2013-2).

References

1. Murray HH (2007) Applied clay mineralogy. Elsevier, The Netherlands
2. Alvarez A, Santarem J, Esteban-Cubillo A, Aparicio P (2011) In: Galán E, Singer A (eds) Developments in palygorskite–sepiolite Research: a new look at these materials, 1st edn. Elsevier, Amsterdam
3. Hitzky ER, Aranda P, Alvarez A, Santarem J, Esteban-Cubillo A (2011) In: Galán E, Singer A (eds) Developments in palygorskite–sepiolite Research. A new look at these materials, 1st edn. Elsevier, Amsterdam
4. Rodriguez-Lazcano Y, Correcher V, Garcia-Guinea J (2013) Thermo- and cathodoluminescence properties of lepidolite. Spectrochim Acta A 113:281–285

5. Garcia-Guinea J, Correcher V, Rodriguez-Lazcano Y, Crespo-Feo E, Prado-Herrero P (2010) Light emission bands in the radioluminescence and thermoluminescence spectra of kaolinite. Appl Clay Sci 49:306–310
6. Correcher V, Garcia-Guinea J, Crespo-Feo E, Rodriguez-Lazcano Y, Prado-Herrero P (2010) Dose–response of thermoluminescence in natural kaolinite. Thermochim Acta 503–504:12–15
7. Bulur E (2008) Preliminary OSL studies on beige sepiolites. Radiat Prot Dosim 131(3):390–393
8. McKeever SWS (1985) Thermoluminescence of solids. Cambridge University Press, New York
9. Kalceff MAS, Phillips MR (1995) Cathodoluminescence microcharacterization of the defect structure of quartz. Phys Rev B 52(5):3122–3134
10. Correcher V, Garcia-Guinea J (2001) On the luminescence properties of adularia feldspar. J Lumin 93:303–312
11. Sanchez del Rio M, García-Romero E, Suarez M, da Silva I, Fuentes-Montero L, Martínez-Criado G (2011) Variability in sepiolite: diffraction studies. Am Miner 96:1443–1454
12. Brauner K, Presinger A (1956) Struktur und Entstehung des Sepioliths. Tschermak's Miner Petrogr Mitt. 6(1–2):120–140
13. Suarez M, Garcia-Romero E (2012) Variability of the surface properties of sepiolite. Appl Clay Sci 67–68:72–82
14. Garcia-Romero E, Suarez M (2013) Sepiolite–palygorskite: textural study and genetic considerations. Appl Clay Sci 86:129–144
15. Yalcin H, Bozkaya O (2011) In: Galán E, Singer A (eds) Developments in palygorskite–sepiolite Research. A new outlook on these nanomaterials. Developments in clay science, 3rd edn. Elsevier, Amsterdam
16. Galán E, Pozo M (2011) In: Galán E, Singer A (eds) Developments in palygorskite–sepiolite Research. A new outlook on these nanomaterials. Developments in clay science, 3rd edn. Elsevier, Amsterdam
17. Bøtter-Jensen L, Duller GAT (1992) A new system for measuring optically stimulated luminescence from quartz samples. Nucl Tracks Radiat Meas Part D 20:549–553
18. Correcher V, Delgado A (1998) On the use of natural quartz as transfer dosemeter in retrospective dosimetry. Radiat Meas 29:411–414
19. Garcia-Guinea J, Correcher V (2000) Luminescence spectra of alkali feldspars: influence of crushing on the ultraviolet emission band. Spectrosc Lett 33:103–113
20. Garcia-Romero E, Suarez M (2014) Sepiolite-palygorskite polysomatic series: oriented aggregation as a crystal growth mechanism in natural environments. Am Miner 99:1653–1661
21. Tauler E, Proenza JA, Gali S, Lewis JF, Labrador M, Garcia-Romero E, Suarez M, Longo F, Bloise G (2009) Ni-sepiolite-falcondoite in garnierite mineralization from the Falcondo Ni-laterite deposit, Dominican Republic. Clay Miner 44:435–454
22. Post JE, Bish DL, Heaney PJ (2007) Synchrotron powder X-ray diffraction Study of the structure and dehydration behavior of sepiolite. Am Miner. 92:91–97
23. Miura A, Nakazawa K, Takei T, Kumada N, Kinomura N, Ohki R, Koshiyama H (2012) Acid-, base-, and heat-induced degradation behavior of Chinese sepiolite. Ceram Int 38:4677–4684
24. Correcher V, Garcia-Guinea J, Martin-Fernandez C, Can N (2011) Thermal effect on the cathodo- and thermoluminescence emission of natural topaz ($Al_2SiO_4(F, OH)_2$). Spectrosc Lett 44:486–489
25. Garcia-Guinea J, Correcher V, Sanchez-Munoz L, Finch AA, Hole DE, Townsend PD (2007) On the luminescence emission band at 340 nm of stressed tectosilicate lattices. Nucl Instrum Methods A 580:648–651
26. Gorobets BS, Grojine AA (2002) Luminescent spectra of minerals. RPC VIMS, Moscow
27. Itoh N, Stoneham D, Stoneham AM (2002) Ionic and electronic processes in quartz: mechanisms of thermoluminescence and optically stimulated luminescence. J Appl Phys 92:5036–5044
28. Martini M, Paleari A, Spinolo G, Vedda A (1995) Role of $[AlO_4]^\circ$ centers in the 380 nm thermoluminescence of quartz. Phys Rev B 52:138–142
29. Sanchez-Munoz L, Correcher V, Garcia-Guinea J, Delgado A (2007) Luminescence at 400 and 440 nm in sanidine feldspar from original and X-ray-induced defects. Nucl Instrum Methods A 580:679–682
30. Speit B, Lehmann G (1982) A comparative study of thermoluminescence and isothermal destruction of radiation defects in feldspars. J Lumin 27:127–136
31. Thurkhin AN (1992) Excitons in SiO2—a review. J Non-Cryst Solids 149(1–2):32–45
32. Garcia-Guinea J, Correcher V, Rodriguez-Badiola E (2001) Analysis of luminescence spectra of leucite ($KAlSiO_4$). Analyst 126:911–916
33. Prescott JR, Fox PJ (1993) 3-dimensional thermoluminescence spectra of feldspars. J Phys D 26:2245–2254
34. Garcia-Guinea J, Fernandez-Cortes A, Alvarez-Gallego M, Garcia-Anton E, Casas-Ruiz M, Blazquez-Perez D, Teijon O, Cuezva S, Correcher V, Sanchez-Moral S (2013) Leaching of uranyl-silica complexes from the host metapelite rock favoring high radon activity of subsoil air: case of Castañar cave (Spain). J Radioanal Nucl Chem 298:1567–1585
35. Gomez-Gonzalez MA, Garcia-Guinea J, Garrido F, Townsend PD, Marco JF (2015) Thallium and manganese complexes involved in the luminescence emission of potassium-bearing aluminosilicates. J Lumin 159:197–206
36. Krbetschek MR, Goetzes J, Dietrich A, Trautmann T (1997) Spectral information from minerals relevant for luminescence dating. Radiat Meas 27:695–748
37. Faye GH (1969) The optical absorption spectrum of tetrahedrally bonded Fe^{3+} in orthoclase. Can Mineral 10:112–117
38. Poolton NRJ, Bøtter-Jensen L, Johnsen O (1996) On the relationship between luminescence excitation spectra and feldspar mineralogy. Radiat Meas 26(1):93–101
39. Correcher V, Sanchez-Munoz L, Garcia-Guinea J, Delgado A (2007) Natural blue thermoluminescence emission of the recently fallen meteorite in Villalbeto de la Peña (Spain). Nucl Instrum Methods A 580:637–640
40. Chen R, McKeever SWS (1997) Theory of Thermoluminescence and Related Phenomena. World Scientific Publishing, Singapore
41. Gonzalez PR, Furetta C, Marcazzo J, Cruz-Zaragoza E, Cruz LP (2013) Determination of kinetics parameters of the main glow peaks for KMgF3: lu and LiF: Mg phosphors after long-term high temperature storage. Appl Radiat Isot 79:67–72
42. Furetta C, Guzman S, Ruiz B, Cruz-Zaragoza E (2011) The initial rise method extended to multiple trapping levels in thermoluminescent materials. Appl Radiat Isot 69:346–349
43. Correcher V, Gomez-Ros JM, Garcia-Guinea J (2004) Radiation effect on the 400 nm-thermoluminescence emission of a potassium rich feldspar. Radiat Meas 38(4–6):689–693
44. Garcia-Guinea J, Pitalua F, Correcher V, Sanchez-Munoz L, Valle-Fuentes FJ, Lopez-Arce P (2004) Thermoluminescent properties of an albite from Minas Gerais (Brazil). Bol Soc Esp Ceram 43(2):115–118